COMPONENT PART NOTICE

THIS PAPER IS A COMPONENT PART OF THE FOLLOWING COMPILATION REPORT:

TITLE: Transactions of the Army Conference on Applied Mathematics and Computing (2nd) Held at Washington, DC on 22-25 May 1984.

TO ORDER THE COMPLETE COMPILATION REPORT, USE AD-A154 047.

THE COMPONENT PART IS PROVIDED HERE TO ALLOW USERS ACCESS TO INDIVIDUALLY AUTHORED SECTIONS OF PROCEEDING, ANNALS, SYMPOSIA, ETC. HOWEVER, THE COMPONENT SHOULD BE CONSIDERED WITHIN THE CONTEXT OF THE OVERALL COMPILATION REPORT AND NOT AS A STAND-ALONE TECHNICAL REPORT.

THE FOLLOWING COMPONENT PART NUMBERS COMPRISE THE COMPILATION REPORT:

AD#: P004 902 thru P004 958 AD#: ____

AD#: ____ AD#: ____

AD#: ____ AD#: ____

Accession For	
NTIS GRA&I	☑
DTIC TAB	☐
Unannounced	☐
Justification	
By	
Distribution/	
Availability Codes	
Dist	Avail and/or Special
A-1	

DTIC FORM MAR 85 463

OPI: DTIC-TID

AD-P004 929

KINEMATIC HARDENING APPLIED TO NON-PROPORTIONAL LOADING

Charles S. White
First Lieutenant

Army Materials and Mechanics Research Center
Watertown, Massachusetts 02172

Abstract

A series of critical experiments in the determination of a plastic flow rule is re-examined using kinematic hardening. Non-proportional loading experiments on thin-walled, aluminum tubes were conducted by Budiansky, Dow, Peters, and Shepherd in 1951 to determine whether plastic flow exhibits behavior consistent with the physical, slip theory of plasticity or with the phenomenological, J_2 flow and deformation theories. Their results were mixed since none of these theories predict the full range of exhibited, material behavior. Pan and Rice have sparked recent interest in these experiments by introducing a slight rate dependence into slip theory. Through a judicious choice of a strain rate sensitivity parameter they match the experiments reasonably well.

This ~~note~~ article reports on the comparison of these experiments against the predictions of a flow rule based on the Prager/ Ziegler kinematic hardening theory. Both shear and axial strains are predicted for a variety of load histories. Results show good agreement between theory and experiment. The implications to buckling and instability analysis are briefly discussed.

I. INTRODUCTION

In this note a brief reassessment of some experiments [1] on plastic flow rules will be made in light of the results predicted using Prager/Ziegler kinematic hardening. First the experiments will be described with the original comparisons using the models of J_2 deformation and flow theories (isotropic hardening) and slip theory. Then the recent paper by Pan and Rice [2] employing rate sensitivity in the slip theory will be shown to improve the modeling. Finally some recent calculations using simple kinematic hardening will be presented and discussed.

At the First National Congress of Applied Mechanics in 1951 the results of some nonproportional loading experiments on thin wall tubular test specimens were presented. Budiansky, Dow, Peters, and Shepherd [1] conducted tests at NACA labs at Langley Field to investigate the behavior of plastic flow near the point of a change in loading direction. They compressed tubes of 14S-T4 aluminum alloy into the plastic range to strains of about 0.5% then abruptly changed the loading path and continued loading at a fixed ratio of axial stress increment to shear stress increment, $d\sigma/d\tau$. Their intent was to look at shear and axial strain response just after this loading corner. The simple plasticity theories in use at that time predict quite different strain behavior. The J_2 isotropic, flow theory contains a smooth yield surface so it predicts that the initial shear strain response would be elastic at a change in the loading direction.

The J_2 deformation theory and the then recently proposed slip theory predict the immediate accumulation of plastic flow. They both predict a tangent modulus which is reduced from its elastic value by the formation of a corner on the yield surface. By determining which theory better approximated the experiments, the authors hoped to explain why plastic buckling experiments agreed better with calculations using a reduced tangent modulus while the body of experimental evidence had supported the model of a smooth yield surface.

Their results are not repeated here in detail except to describe the general trends and the authors conclusions. In each specimen the initial shear response was elastic. For all ratios of $d\sigma/d\tau$ the elastic shear strain accounted for all the measured shear strain just after the loading corner. This observation is in accordance with J_2 isotropic, flow theory or any flow theory having a smooth yield surface.

For continued straining the results did not favor one theory over another. The experiments showed shear response that was "softer" than predicted by isotropic hardening flow theory but was "stiffer" than predicted by slip or deformation theories. The experimental results fell between the predictions.

For most of the cases, the continued accumulation of plastic strain after the loading corner is underestimated by these theories. One explanation lies with the treatment of the behavior of this aluminum alloy as rate independent at room temperature. The tests were run at a very slow strain rate ($\sim 10^{-6}$ sec $^{-1}$) and a component of creep strain might be expected. This would lead to an increase in the axial strain over the predictions of the rate independent theory.

II. RATE DEPENDENT SLIP THEORY

In a 1983 paper by Pan and Rice [2], recent interest was shown in these experiments. Rate dependence was used to improve the predictions of slip theory. Pan and Rice investigated the implications of introducting a slight rate dependence into the simple slip theory of Batdorf and Budiansky [3]. The original assumption was that the shear strain on any slip system in a crystal is a function only of the maximum resolved shear stress on that system over the loading history. This leads to a rate independent theory for the macroscopic constitutive behavior when integrated over all slip directions and slip systems.

Pan and Rice assumed that the microscopic behavior is slightly rate dependent through a non-linear viscous relation:

$$\dot{\gamma} = \dot{a}\left(\frac{\tau}{g(\gamma)}\right)^{1/m} \qquad (1)$$

where $\dot{\gamma}$ is the plastic shearing rate, m is the plastic strain rate sensitivity, $\dot{a}$ is the reference plastic shearing rate and $g(\gamma)$ is a function of the current state. Note that $g(\gamma)$ is just the function for τ when $\dot{\gamma} = \dot{a}$.

Several values for m were chosen since separate tests for strain rate sensitivity had not been conducted. The value of m which gave the best matching with the nonproportional tests was 0.03. This value is a little higher than one would normally expect for aluminum at room temperature [2].

Pan and Rice show results for 3 of the 6 experiments conducted by Budiansky et. al. In each case they show that the introduction of rate dependence can greatly increase the agreement of slip theory with the experiments. Their results are repeated here in Figures 1-3. Note that the original results of Budiansky et. al. are also plotted. An initial elastic shear stress-strain response is predicted at the loading corner in accordance with observations. The continued deformation is also predicted quite well although there is some divergence between theory and experiment at higher strain. By judicious choice of the strain rate sensitivity parameter, rate dependent slip theory can be shown to give a good description of these nonproportional loading experiments.

For detailed calculations on buckling and other instability phenomena the information obtained from these types of tests are crucial. The predicted loads are very sensitive to the transverse stiffness after longitudinal plastic straining. The rate dependent slip theory is shown to provide a good model which can match experiments quite well by adjusting the strain rate sensitivity. This sort of a microscopically based model is useful when considering simple geometries and homogenous stress states but is far too computationally expensive for use in general analysis such as might be conducted using a finite element code. It is for this reason that this author has examined simple, kinematic hardening in the context of nonproportional loading.

III. KINEMATIC HARDENING

Budiansky et. al. [1] remarked that their data might be best correlated by a linear flow theory whose loading function gives a higher curvature to the loading surface at the prestress point that does isotropic hardening. The simple kinematic hardening model proposed by Prager [4] satisfies just such a set of conditions, the curvature being given by that of the initial yield surface. Prager first introduced the concept of a translating yield surface in 1955 so the model was not available to Budiansky et. al. at the time they analyzed these experiments. It appears that nonproportional loading experiments of this type have never been examined with the kinematic hardening model. After the early 1950's, the experimental emphasis in biaxial plasticity turned away from studying flow rules to plotting yield loci. Kinematic hardening concepts have been successfully used to describe some of the phenomena associated with yield surface movement but as a flow rule the theory has not been subject to the same experimental scrutiny.

Without going into a detailed discussion of the development of this phenomenological theory, a few remarks are appropriate. The theory considered here is that proposed by Prager [4] and later modified by Ziegler [5]. Restricting ourselves to small strains we consider an initial yield surface of the von Mises type which retains its size and shape but translates without rotation during plastic straining. The flow rule is associative and the evolution law for the position, in stress space, of the yield surface center is given by

$$\dot{\underset{\sim}{\alpha}} = \mu(\underset{\sim}{S}-\underset{\sim}{\alpha}) \tag{2}$$

where $\underset{\sim}{S}$ is the stress deviator and μ is the scalar function, derivable from the consistency condition, which describes the hardening behavior. This theory was applied to the experiments of Budiansky et. al. A power law form was applied to match the standard uniaxial stress strain curve in compression given in [2].

$$\varepsilon^{p} = c\left(\frac{\sigma}{\sigma_{o}} - 1\right)^{n}$$

$$\text{where} \quad \sigma_{o} = 25 \text{ ksi}, \quad n = 3.33, \quad c = 0.0317 \tag{3}$$

These values gave a very good match to the compression experiment and provided easy evaluation of the stiffness at any strain level during the nonproportional test. In order to account for slight differences in material properties between specimens, we adopt the same approach as Budiansky et. al. During the pure compressive loading portion of each test the uniaxial stress strain curve was compared with of the standard curve. The ratio, denoted by λ, of the stress given by the standard curve to that of the individual specimens during the compressive loading was used to modify the expression above. They assumed that the plastic strain would be a function of λ times σ.

$$\varepsilon^p = c \left(\frac{\lambda\sigma}{\sigma_o} - 1 \right)^n \tag{4}$$

where

$$\lambda = \frac{(\sigma_x)\ \text{standard curve}}{(\sigma_x)\ \text{specimen}}$$

This allowed the same uniaxial stress strain relation to be used for all the specimens even though small differences in the flow stress level were exhibited between specimens. The values of λ were determined from the compressive loading portion of the tests. They are tabulated in [1].

The kinematic hardening relations were coded using a one-step, Euler explicit integration scheme. The step size was varied to study error accumulation. Increasing the number of equal steps from 100 to 1000 changed the final plastic strain by less than 1%. Since error varies inversely with step size in a linear fashion for explicit Euler 1000 steps was considered sufficient for predictions within experimental accuracy. The same procedure was also used to integrate small strain, isotropic hardening relations for comparison.

The six loading histories tested by Budiansky et. al. were considered. They are shown schematically in Figure 4. Notice that the ratios of $d\sigma/d\tau$ for continued loading varied from +1.91 to -1.13. This covered the range from total loading to elastic unloading.

Figures 5-10 show the results for the isotropic and kinematic models compared to the experimental data. Shear stress versus plastic shear strain and versus the increase in plastic axial strain are plotted. Notice in each case that the kinematic hardening model matches the shear strain response very well. The kinematic model accurately predicts the softer response for shear following axial extension. The most interesting point is that the kinematic model does such a good job of predicting when plastic flow will recommence for the two cases when the loading trajectories go back through the elastic zone of the kinematic and isotropic models ($d\sigma/d\tau = -0.656, -1.13$). This is clearly seen from Figure 4 where the shear stress levels for the intersection of the loading path with the yield surface is much different for the two models. The kinematic model yields results much closer to experimental observation. This is an example of how non-proportional loading tests are valuable and necessary in constructing a flow rule.

An interesting behavior is predicted for the case $\frac{d\sigma}{d\tau}$ = -1.13. Figure 10 shows that the axial strain changes direction for the kinematic hardening model. This is a result of the yield surface translating far enough to the right that the loading point has moved around to the left half of the yield surface. Unfortunately, the experiments were not run far enough to show whether this behavior would occur. The kinematic model does a good job of predicting these axial strains. The kinematic hardening model does better than the other theories applied to this problem. It predicts more axial straining than the other theories and provides a good overall match with experiments.

IV. CONCLUSIONS

The calculations presented here demonstrate that although most plasticity theories yield identical results when applied to proportional load histories, the change in loading direction can greatly affect the predicted material response. In particular, simple kinematic hardening was shown to provide much better agreement with experiment than isotropic hardening. In light of the overwhelming use of isotropic hardening in even this small strain regime the analyst must use care in applying a particular hardening model. The results presented here indicate that kinematic hardening should be a more suitable model for buckling or bifurcation studies. In fact, Tvergaard [6] showed that large strain, kinematic hardening provided good results for biaxial necking.

References:

1. Budiansky, B., Dow, N., Peters, R. and R. Shepherd, "Experimental Studies of Polyaxial Stress-Strain Laws of Plasticity", Proc. 1st. U. S. Natl. Congr. Appl. Mech., 1951, pp. 503-512.

2. Pan, J., and J. R. Rice, Int. J. Solids Structures, Vol. 19, 1983, pp. 973-987.

3. Batdorf, S. B. and B. Budiansky, NACA TN 1871, April 1949.

4. Prager, W., J. Appl. Mech., Vol. 23, 1956, pp. 493-496.

5. Ziegler, H., Quar. Appl. Math., Vol. 17, 1959, pp. 55-65.

6. Tvergaard, V., Int. J. Mech. Sci., Vol. 20, 1978, pp. 651-658.

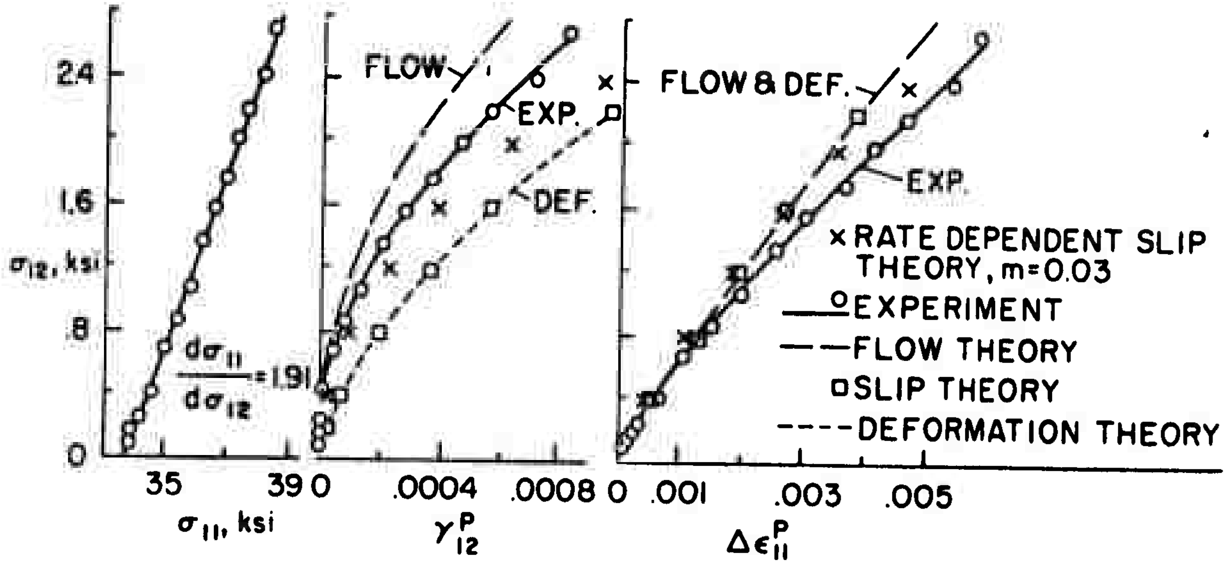

Figure 1. Results of Pan and Rice [2] showing comparison of the various theories with the experiments of Budiansky et. al. [1] for $d\sigma/d\tau = 1.91$. Note that they use the notation of $\sigma_{11} = \sigma$, and $\sigma_{12} = \tau$.

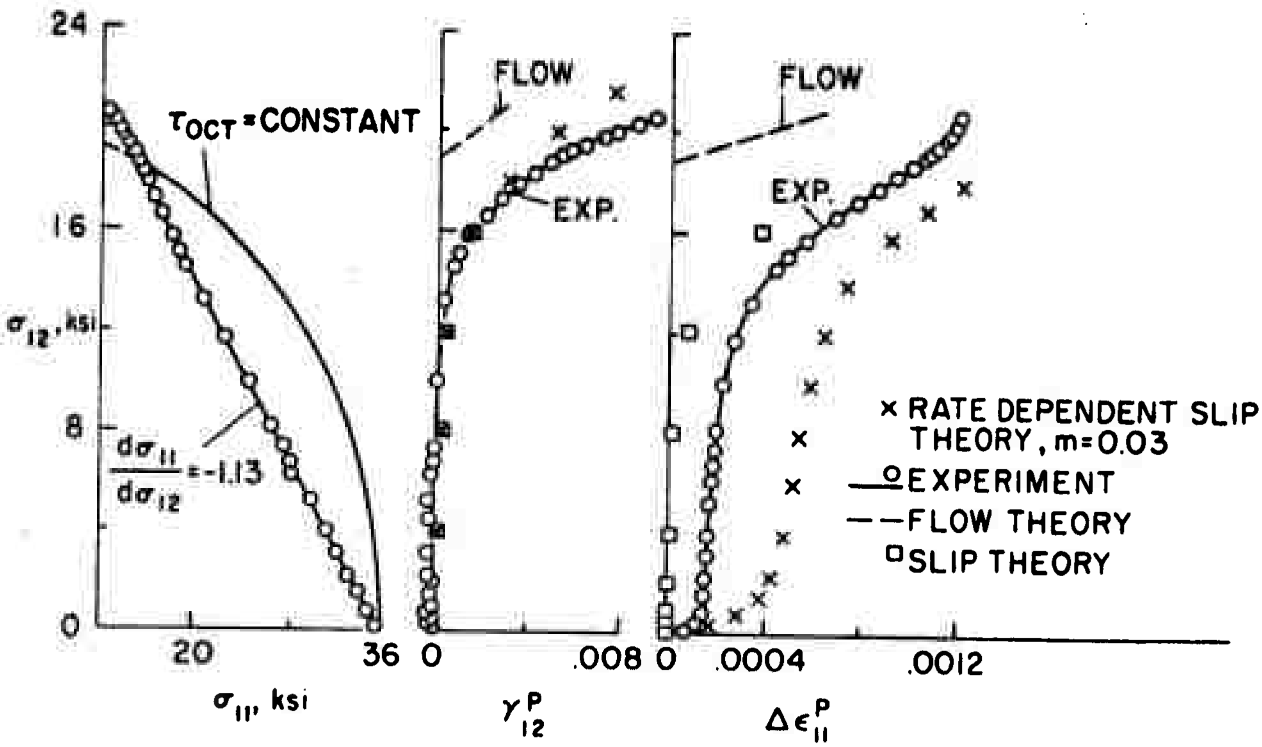

Figure 2. Results of Pan and Rice [2] showing comparisons among the various theories for $d\sigma/d\tau = -1.13$.

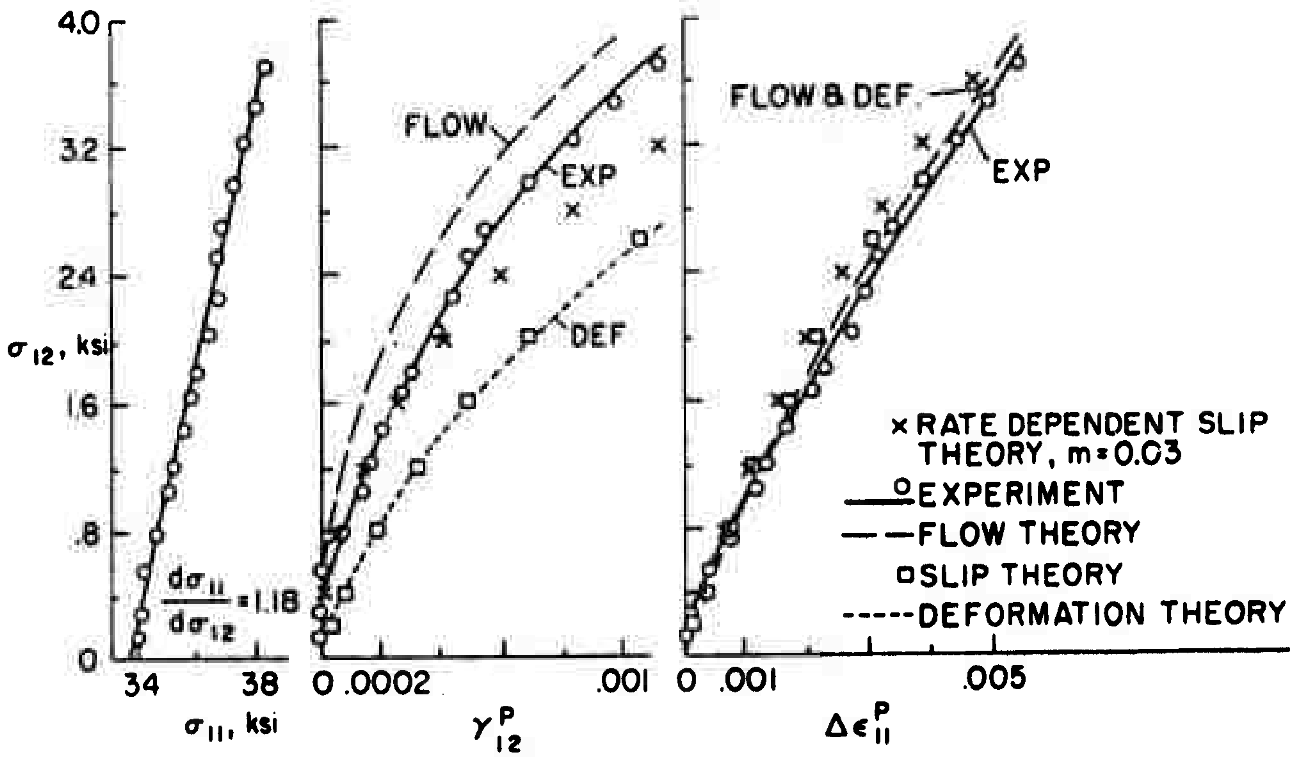

Figure 3. Results of Pan and Rice [2] showing comparisons among the various theories for $d\sigma/d\tau = 1.18$.

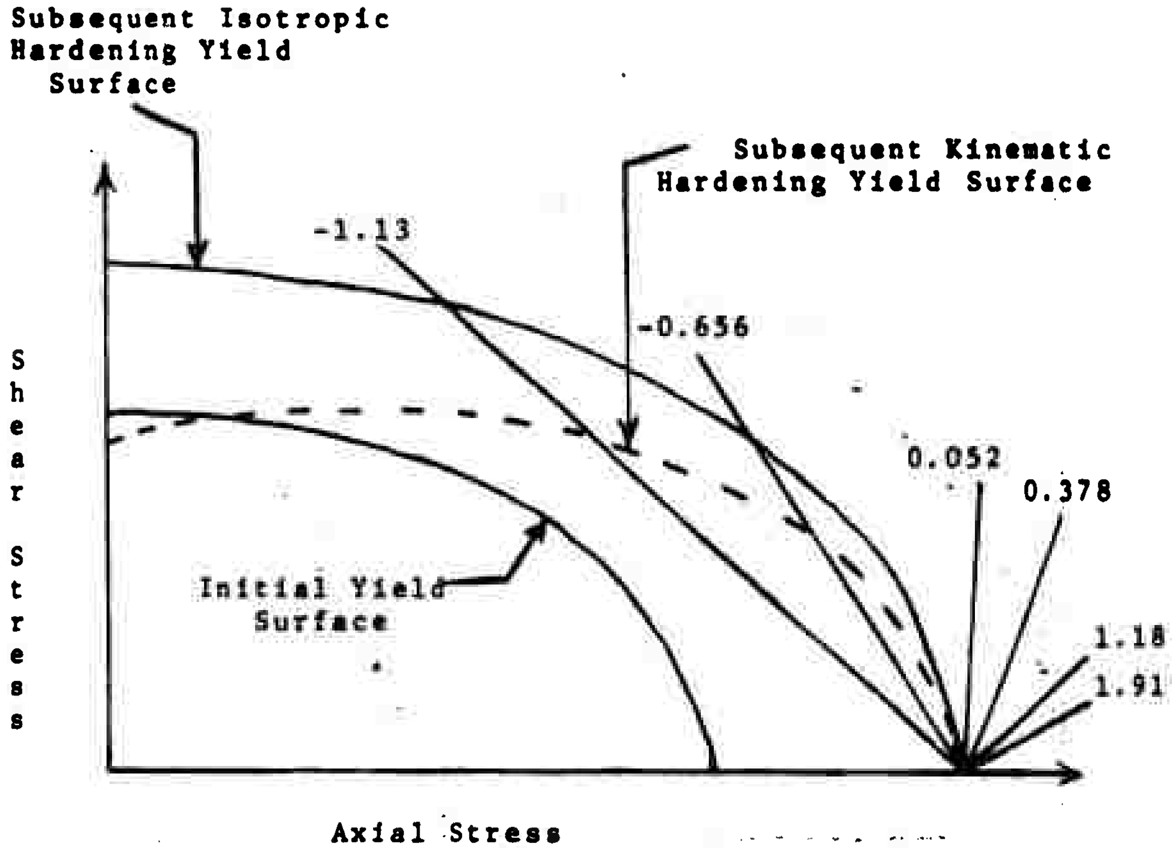

Figure 4. Comparison of initial yield surface with that predicted after initial axial compression using both isotropic and kinematic hardening. The subsequent loading trajectories are also shown with the corresponding values of $d\sigma/d\tau$.

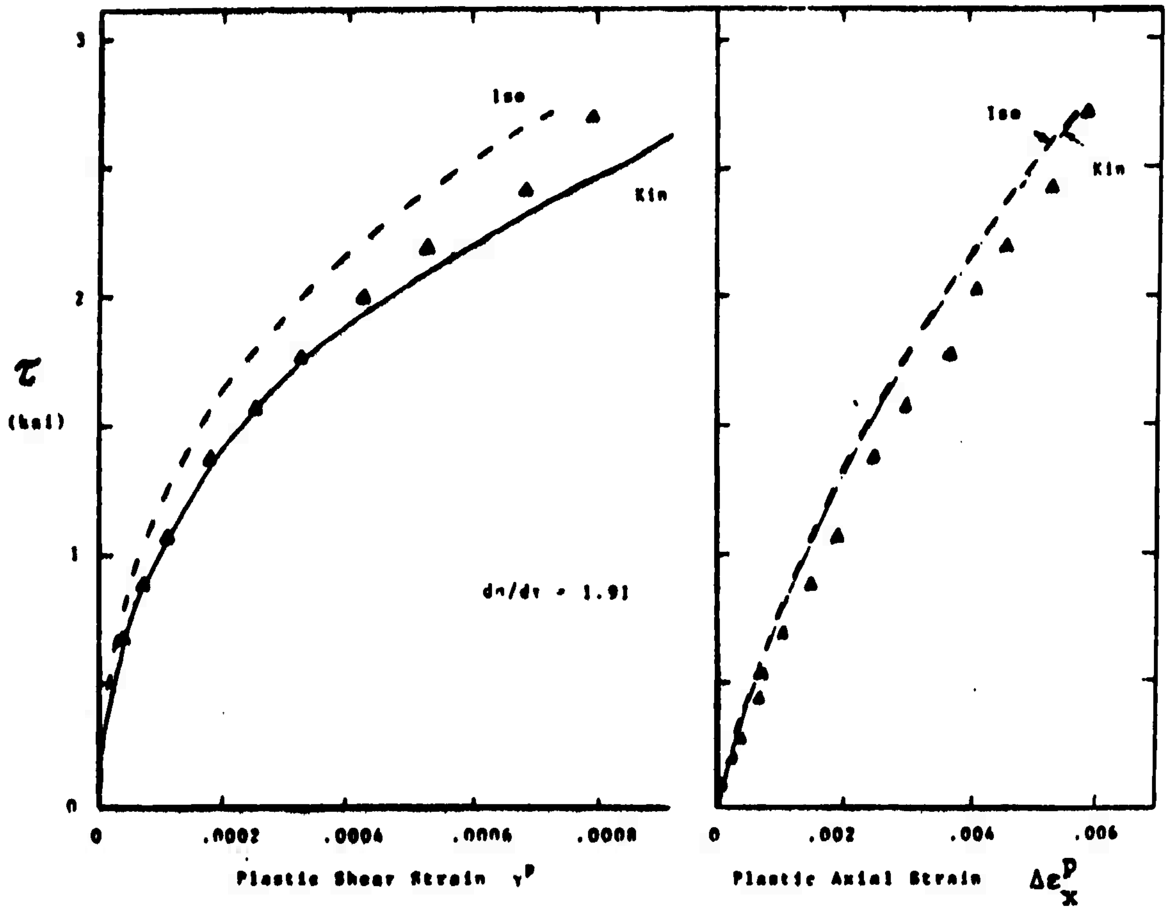

Figure 5. Comparison of isotropic and kinematic hardening flow theories with experiments of Budiansky et. al. [1]. Filled triangles indicate measurements of plastic flow along $d\sigma/d\tau = 1.91$ after initial axial compression.

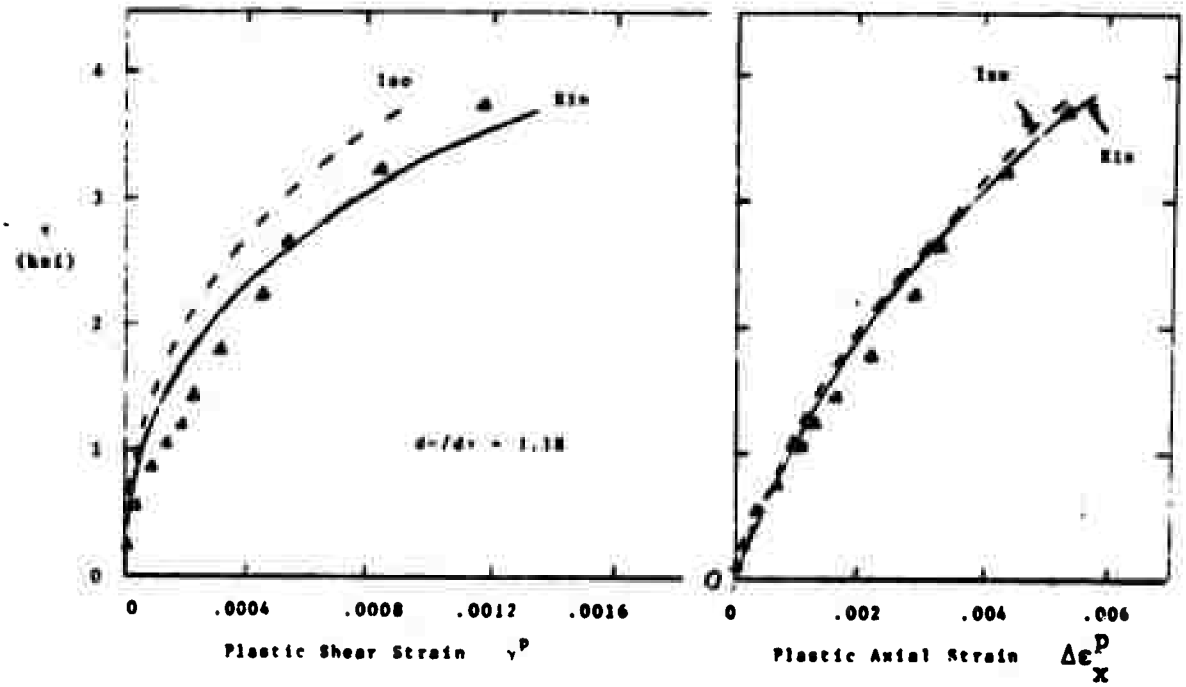

Figure 6 . Comparison of isotropic and kinematic hardening flow theories with experiments of Budiansky et. al. [1]. Filled triangles indicate measurements of plastic flow along $d\sigma/d\tau = 1.18$ after initial axial compression.

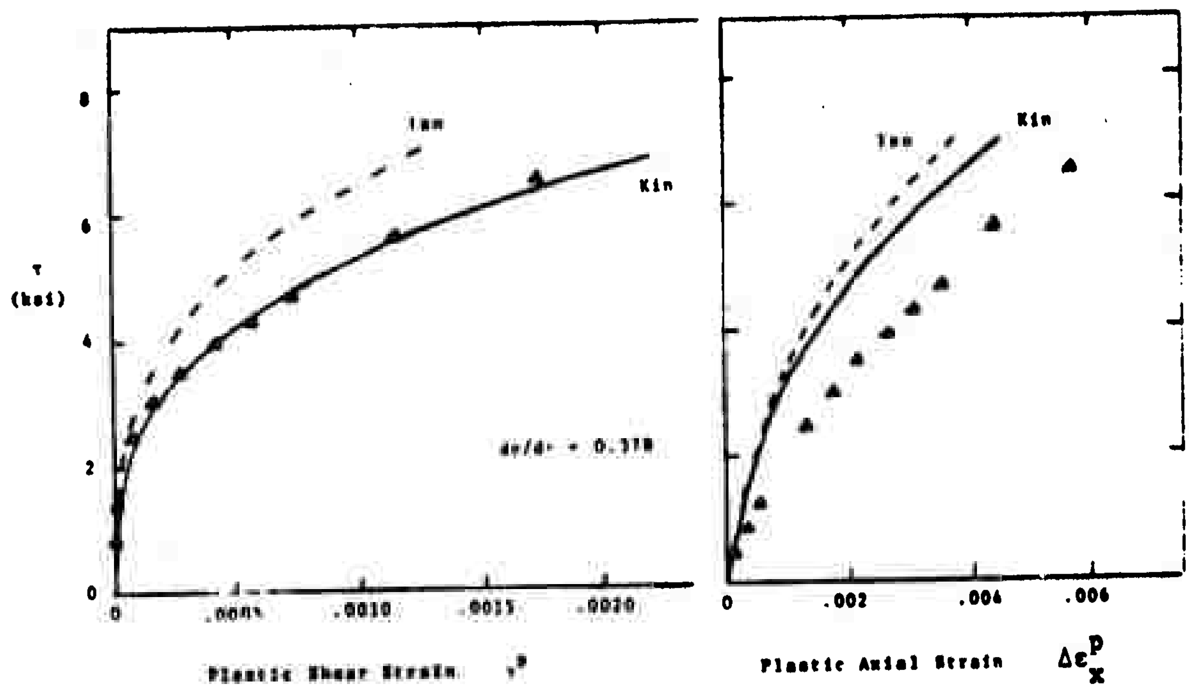

Figure 7. Comparison of isotropic and kinematic hardening flow theories with experiments of Budiansky et. al. [1]. Filled triangles indicate measurements of plastic flow along dσ/dτ = 0.378 after initial axial compression.

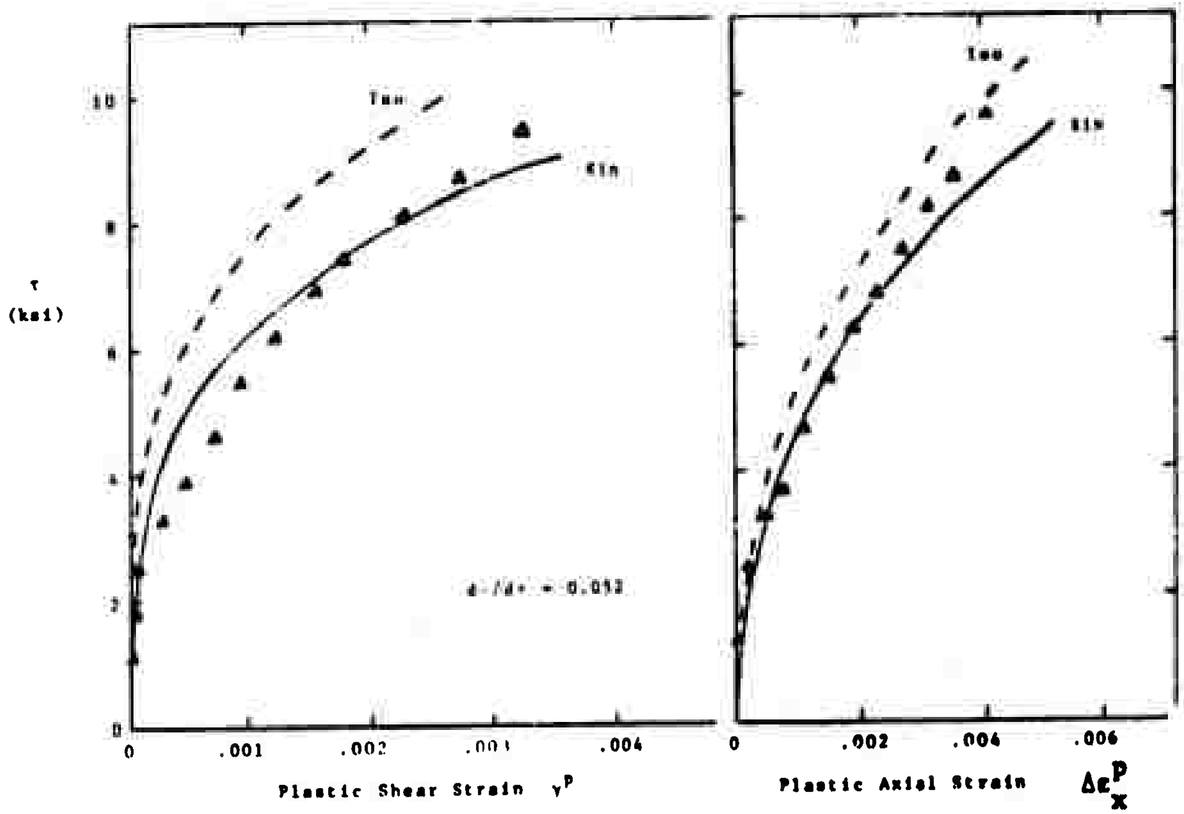

Figure 8. Comparison of isotropic and kinematic hardening flow theories with experiments of Budiansky et. al. [1]. Filled triangles indicate measurements of plastic flow along $d\sigma/d\tau = 0.052$ after initial axial compression.

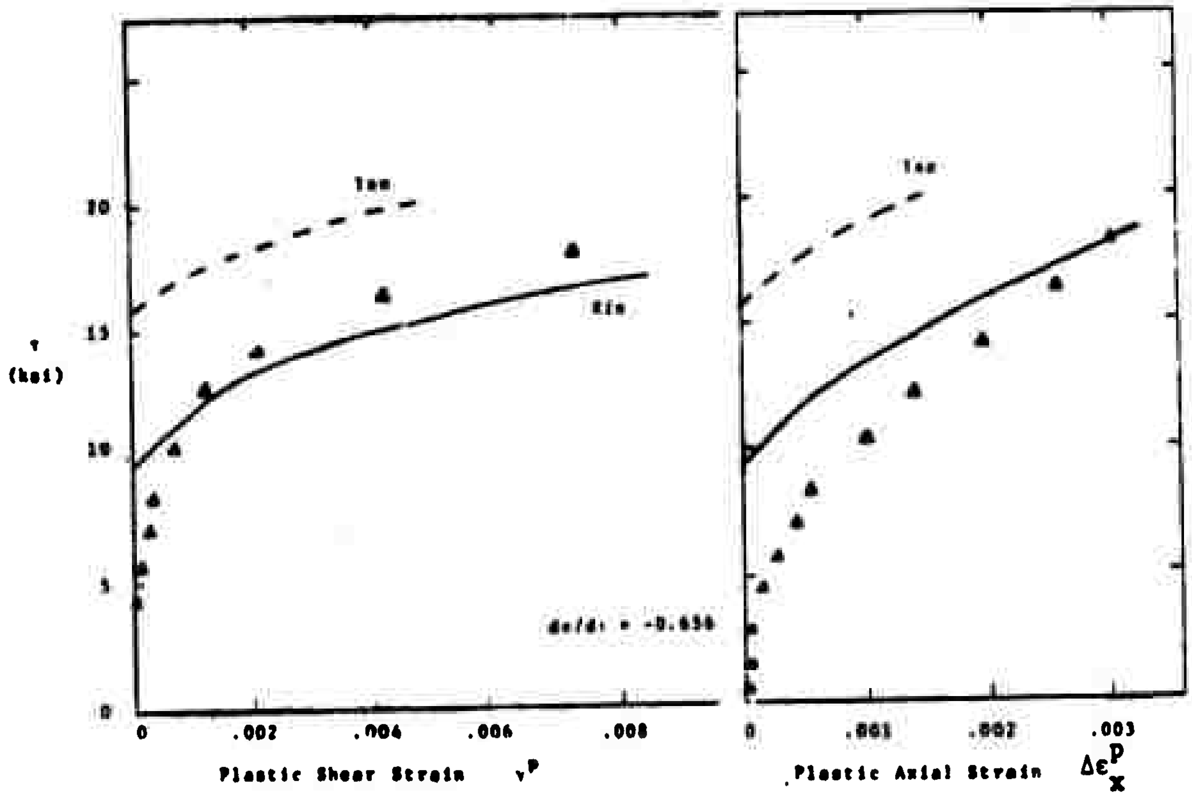

Figure 9 . Comparison of isotropic and kinematic hardening flow theories with experiments of Budiansky et. al. [1]. Filled triangles indicate measurements of plastic flow along dσ/dτ =-0.656 after initial axial compression.

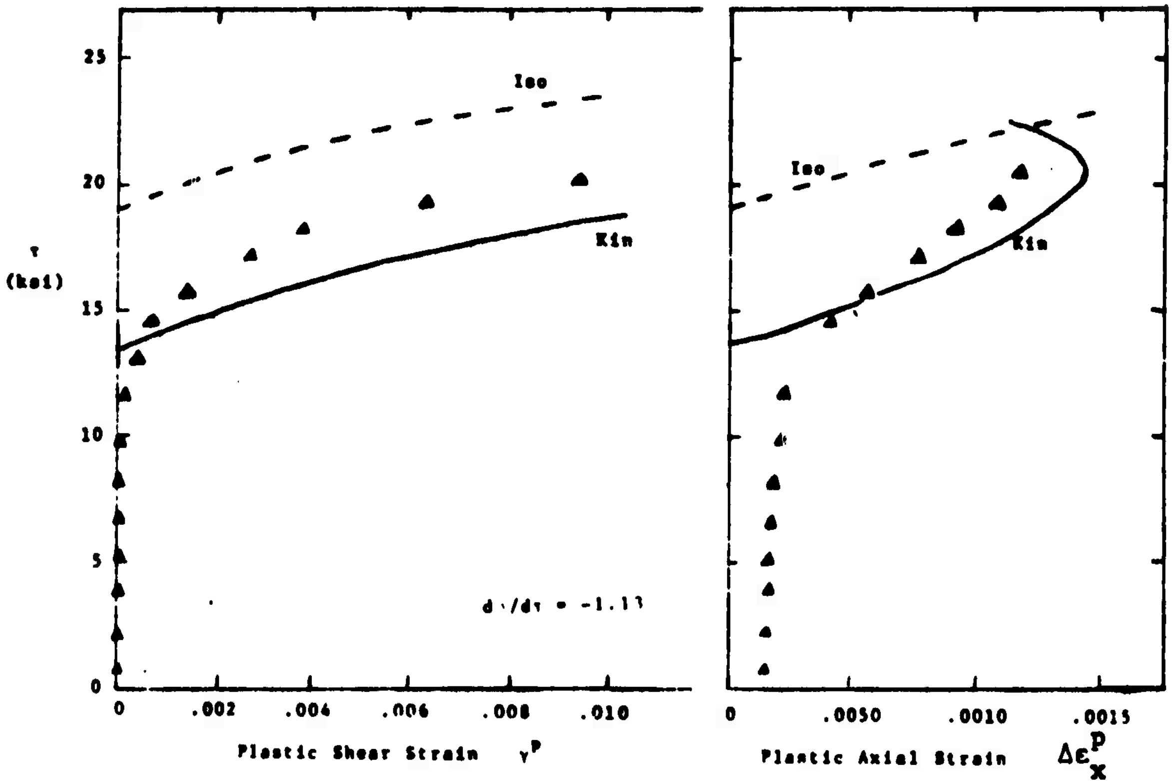

Figure 10. Comparison of isotropic and kinematic hardening flow theories with experiments of Budiansky et. al. [1]. Filled triangles indicate measurements of plastic flow along $d\sigma/d\tau = -1.13$ after initial axial compression.